Geometry of river networks. III. Characterization of component connectivity

Peter Sheridan Dodds[1,2,*] and Daniel H. Rothman[2,†]
[1]*Department of Mathematics, Massachusetts Institute of Technology, Cambridge, Massachusetts 02139*
[2]*Department of Earth, Atmospheric and Planetary Sciences, Massachusetts Institute of Technology, Cambridge, Massachusetts 02139*

(Received 18 May 2000; revised manuscript received 18 September 2000; published 27 December 2000)

Essential to understanding the overall structure of river networks is a knowledge of their detailed architecture. Here we explore the presence of randomness in river network structure and the details of its consequences. We first show that an averaged view of network architecture is provided by a proposed self-similarity statement about the scaling of drainage density, a local measure of stream concentration. This scaling of drainage density is shown to imply Tokunaga's law, a description of the scaling of side branch abundance along a given stream, as well as a scaling law for stream lengths. We then consider fluctuations in drainage density and consequently the numbers of side branches. Data are analyzed for the Mississippi River basin and a model of random directed networks. Numbers of side streams are found to follow exponential distributions, as are intertributary distances along streams. Finally, we derive a joint variation of side stream abundance with stream length, affording a full description of fluctuations in network structure. Fluctuations in side stream numbers are shown to be a direct result of fluctuations in stream lengths. This is the last paper in a series of three on the geometry of river networks.

DOI: 10.1103/PhysRevE.63.016117 PACS number(s): 64.60.Ht, 92.40.Fb, 92.40.Gc, 68.70.+w

I. INTRODUCTION

This paper follows Refs. [1] and [2] as the last in a series on the geometry of river networks. In the first paper [1], we examined in detail the description of river networks by scaling laws [3–6] and the evidence for universality. Additional introductory remarks concerning the motivation of the overall work were provided in this first paper. In the second paper [2], we addressed distributions of the basic components of river networks, stream segments, and subnetworks. Here we present an analysis complementary to the work of the second paper by establishing a description of how river network components fit together. One may see the second paper as building up and out to global descriptions, whereas the present work travels in the opposite direction, descending to examine the subtle intricacies of network structure. As before, we are motivated by the premise that while relationships of mean quantities are primary in any investigation, the behavior of higher order moments potentially and often do encode significant information.

Our purpose then is to investigate the distributions of quantities which describe the detailed architecture of river networks. We center our attention on Tokunaga's law [7–9], which is a statement about network architecture describing the tributary structure of streams. As in Refs. [1] and [2], we use data from the Scheidegger model of random networks [10] and the Mississippi River, finding the distributions obtained from these two disparate sources to agree very well in form. We are able to set down scaling forms of all distributions studied. We observe a number of distributions to be exponential, therefore requiring only one parameter for their description, and indicating the presence of randomness. As a result, we introduce a dimensionless scale ξ_t which is simply related to the length scale ξ introduced in Ref. [2]. Significantly, we observe the spatial distribution of stream segments to be random, implying that we have reached the most basic description of network architecture.

Tokunaga's law is intimately connected with drainage density ρ, a quantity which will be used throughout the paper. Drainage density is a measure of the stream concentration or, equivalently, how a network fills space. We explore this connection in detail, showing how simple assumptions regarding drainage density lead to Tokunaga's law.

The paper is structured as follows. We define Tokunaga's law, and introduce a scaling law for a specific form of drainage density. We briefly describe Horton's laws for stream number and length and some simple variations. Both stream ordering and Horton's laws are also briefly mentioned; they were covered in more detail in Ref. [2]. We show that the scaling law of drainage density may be taken as an assumption from which all other scaling laws follow. This brings us to the focal point of the paper: the identification of a statistical generalization of Tokunaga's law. We first examine distributions of numbers of tributaries (side streams) and compare these with distributions of stream segment lengths which were shown to be exponential in Ref. [2]. We observe the former distributions also to be exponential, leading to the notion that stream segments are distributed randomly throughout a network. The presence of exponential distributions also leads to the introduction of the characteristic number ξ_t. We then study the variation of tributary spacing along streams so as to understand fluctuations in drainage density, and again find the signature of randomness. Finally, we develop a joint probability distribution connecting the length of a stream with the frequency of its side streams.

*Author to whom correspondence should be addressed; Electronic address: dodds@segovia.mit.edu; URL:http://segovia.mit.edu/
†Electronic address: dan@segovia.mit.edu

TABLE I. Dimensionless Tokunaga ratios for the Mississippi River. The row indices are the absorbing stream orders, while the columns correspond to side stream orders. Each entry is the average number of order ν side streams per order μ absorbing stream to two significant digits.

	$\nu=1$	2	3	4	5	6	7	8	9	10
$\mu=2$	1.7									
3	4.9	1.3								
4	12	3.8	1.1							
5	29	9.1	2.9	1.0						
6	71	23	7.7	3.0	1.2					
7	190	56	19	7.8	3.3	1.1				
8	380	110	39	17	6.9	2.6	1.0			
9	630	170	64	28	11	4.5	3.0	0.60		
10	1100	270	66	29	13	4.3	2.7	1	1	
11	1400	510	120	66	25	12	9	3	1	1

II. DEFINITIONS

For full definitions of stream ordering and Horton's laws, the reader is referred to the first two papers of this series [1,2]. Here, we recall some notation for convenience, introduce some additional terminology, and present Tokunaga's law in more detail.

In discussing network architecture, we will speak of *side streams* and *absorbing streams*. A side stream is any stream that joins into a stream of higher order, the latter being the absorbing stream. We will denote the orders of absorbing and side streams by μ and ν but when referring to an isolated stream or streams where their relative rank is ambiguous, we will write stream order as ω.

Central to our investigation of network architecture is stream segment length. As in Ref. [2], we denote this length by $l_\omega^{(s)}$ for a stream segment of order ω. We will also introduce a number of closely related lengths which describe distances between side streams. When referring to streams throughout we will specifically mean stream segments of a particular order unless otherwise indicated. This is to avoid confusion with the more natural definition of a stream which is the path from a point on a network moving upstream to the most distant source. For an order ω basin, we denote this *main stream length* by l_ω.

Defining a stream ordering on a network allows for a number of well-defined measures of connectivity, stream lengths, and drainage areas. Around a decade after the Strahler-improved stream ordering of Horton appeared [11,12], Tokunaga introduced the idea of measuring side stream statistics [7–9]. This technique arguably provides the most useful measurement based on stream ordering, and only recently received much attention [5,13–15]. The idea is simply, for a given network, to count the average number of order ν side streams entering an order μ absorbing stream. This gives $\langle T_{\mu,\nu}\rangle$, a set of double-indexed parameters for a basin. Note that $\Omega \geqslant \mu > \nu \geqslant 1$, where Ω is the order of the network, so we can view the Tokunaga ratios as a lower triangular matrix. An example for the Mississippi River is shown in Table I [16]. The same data are represented pictorially in Fig. 1 in what we refer to as a *Tokunaga graph*.

Tokunaga made several key observations about these side stream ratios. The first is that because of the self-similar nature of river networks, $\langle T_{\mu,\nu}\rangle$ should not depend absolutely on either of μ or ν but only on the relative difference, i.e., $k=\mu-\nu$. The second is that in changing the value of $k=\mu-\nu$, the $\langle T_{\mu,\nu}\rangle$ must themselves change by a systematic ratio. These statements lead to what we refer to as Tokunaga's law:

$$\langle T_{\mu,\nu}\rangle = \langle T_k\rangle = \langle T_1\rangle (R_T)^{k-1}. \tag{1}$$

Thus only two parameters are necessary to characterize the set of $T_{\mu,\nu}$: T_1 and R_T.

The parameter $T_1 > 0$ is the average number of side streams of one order lower than the absorbing stream, typically on the order of 1.0–1.5. Since these side streams of one order less are the dominant side streams of the basin, their number estimates the basin's breadth. In general, larger values of $\langle T_1\rangle$ correspond to wider basins, while smaller values are in keeping with basins with relatively thinner profiles.

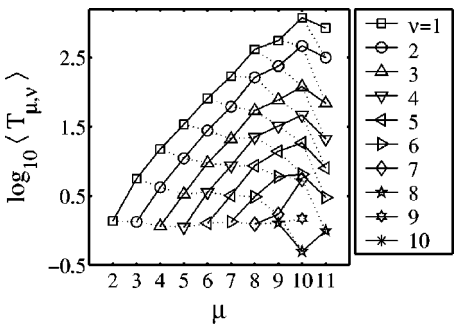

FIG. 1. A Tokunaga graph for the Mississippi River. The values are given in Table I. Each point represents a Tokunaga ratio $\langle T_{\mu,\nu}\rangle$. The solid lines follow variations in the order of the absorbing stream μ, while the dotted lines follow unit increments in both μ and ν, the order of side streams. In comparison, the Tokunaga graph of an exactly self-similar network would have points evenly spaced at $\ln T_1 + (\mu+\nu-1)\ln R_T$ where $1 \leqslant \nu < \mu = 2,3,\ldots,\Omega$, i.e., all lines in the plot would be straight and uniformly spaced, with the dotted lines being horizontal. The nature of deviations in scalings laws for river networks was addressed in Ref. [1].

The ratio $R_T>1$ measures how the density of side streams of decreasing order increases. Thus already inherent in Tokunaga's law is a generalization of drainage density ρ, the usual definition of which is given as follows. For a given region of landscape with area A with streams totalling in length L, $\rho=L/A$, and has the dimensions of an inverse length scale [11]. One may think of ρ as the inverse of the typical distance between streams, i.e., the characteristic scale beyond which erosion cannot more finely dissect the landscape [11]. In principle, the drainage density may vary from landscape to landscape and also throughout a single region. Below, we will turn this observation about Tokunaga's law around to show that all river network scaling laws may be derived from an expanded notion of drainage density.

Even though the number of side streams entering any absorbing stream must of course be an integer, Tokunaga's ratios are under no similar obligation since they are averages. Nevertheless, Tokunaga's law provides a good sense of the structure of a network, albeit at a level of averages. One of our main objectives here is to go further and consider fluctuations about and the full distributions underlying the $\langle T_{\mu,\nu}\rangle$.

As in Ref. [2], we consider the Horton-like law for stream segment lengths:

$$\frac{\langle l_{\omega+1}^{(s)}\rangle}{\langle l_{\omega}^{(s)}\rangle}=R_{l^{(s)}}. \tag{2}$$

As we will show, the form of the distribution of the variable $T_{\mu,\nu}$ is a direct consequence of the distribution of $l_{\omega}^{(s)}$.

III. IMPLICATIONS OF A SCALING LAW FOR DRAINAGE DENSITY

We now introduce a law for drainage density based on stream ordering. We write $\rho_{\mu,\nu}$ for the number of side streams of order ν per unit length of order μ absorbing stream. We expect these densities to be independent of the order of the absorbing stream, and so we will generally use ρ_{ν}. The typical length separating order ν side streams is then $1/\rho_{\nu}$. Assuming self-similarity of river networks, we must have

$$\rho_{\nu+1}/\rho_{\nu}=1/R_{\rho}, \tag{3}$$

where $R_{\rho}>1$, independent of ν.

All river network scaling laws in the planform may be seen to follow from this relationship. Consider an absorbing stream of order μ. Self-similarity immediately demands that the number of side streams of order $\mu-1$ must be statistically independent of μ. This number is of course $\langle T_1\rangle$. Therefore, the typical length of an order μ absorbing stream must be

$$\langle l_{\mu}^{(s)}\rangle=\langle T_1\rangle/\rho_{\mu-1}. \tag{4}$$

Using Eq. (3) to replace $\rho_{\mu-1}$ in the above equation, we find

$$T_1/\rho_{\mu-1}=R_{\rho}T_1/\rho_{\mu-2}. \tag{5}$$

Thus $T_2=R_{\rho}T_1$ and, in general $T_k=(R_{\rho})^{k-1}T_1$. This is Tokunaga's law, and we therefore have

$$R_{\rho}\equiv R_T. \tag{6}$$

Equations (3) and (4) also give

$$\langle l_{\mu}^{(s)}\rangle=T_1/\rho_{\mu-1}=R_{\rho}T_1/\rho_{\mu-2}=R_{\rho}\langle l_{\mu-1}^{(s)}\rangle. \tag{7}$$

On comparison with Eq. (2), we see that the above is our Hortonian law of stream segment lengths, and that

$$R_{\rho}\equiv R_{l^{(s)}}. \tag{8}$$

As $R_{l^{(s)}}$ is the basic length-scale ratio in the problem, we rewrite Eq. (3), our Hortonian law of drainage density, as

$$\rho_{\nu+1}/\rho_{\nu}=1/R_{l^{(s)}}. \tag{9}$$

The above statement becomes our definition of the self-similarity of drainage density.

IV. TOKUNAGA DISTRIBUTIONS

Tokunaga's law relates averages of quantities, and in the remainder of this paper we investigate the underlying distributions from which these averages are made. We are able to find general scaling forms of a number of distributions, and in many cases also identify the basic form of the relevant scaling function.

All investigations are initially carried out for the Scheidegger model, where we may generate statistics of ever-improving quality. We note that the Tokunaga parameters and the Horton ratios are not known analytically. Estimates from previous work [5] find $T_1\simeq 1.35$, $R_{l^{(s)}}=R_T\simeq 3.00$, and $R_n\simeq 5.20$. Data for the present analysis were obtained on $L=10^4$ by $W=3\times 10^3$ lattices with periodic boundaries. Given the self-averaging present in any single instance on these networks, ensembles of ten were deemed sufficient. We also find the same forms for all distributions for the Mississippi data (and for other river networks not presented here). Perhaps the most significant benefit of the simple Scheidegger model is its ability to provide clean distributions whose form we can then search for in real data.

The distribution of $T_{\mu,\nu}$ is well described by an exponential distribution. This can be seen upon inspection of Figs. 2(a) and 2(b). Figure 2(a) shows normalized distributions of $T_{\mu,\nu}$ for $\nu=2$ and varying absorbing stream order $\mu=4$, 5, and 6. These distributions (plus the one for absorbing stream order $\mu=7$) are rescaled and presented in Fig. 2(b). The single form thus obtained suggests a scaling form of the $T_{\mu,\nu}$ distribution is given by

$$P(T_{\mu,\nu})=(R_{l^{(s)}})^{-\mu}F[T_{\mu,\nu}(R_{l^{(s)}})^{-\mu}], \tag{10}$$

where F is an exponential scaling function. However, this only accounts for variations in μ, the order of the absorbing stream.

Figures 3(a) and 3(b) show that a similar rescaling of the distributions may be effected when ν is varied. In this case,

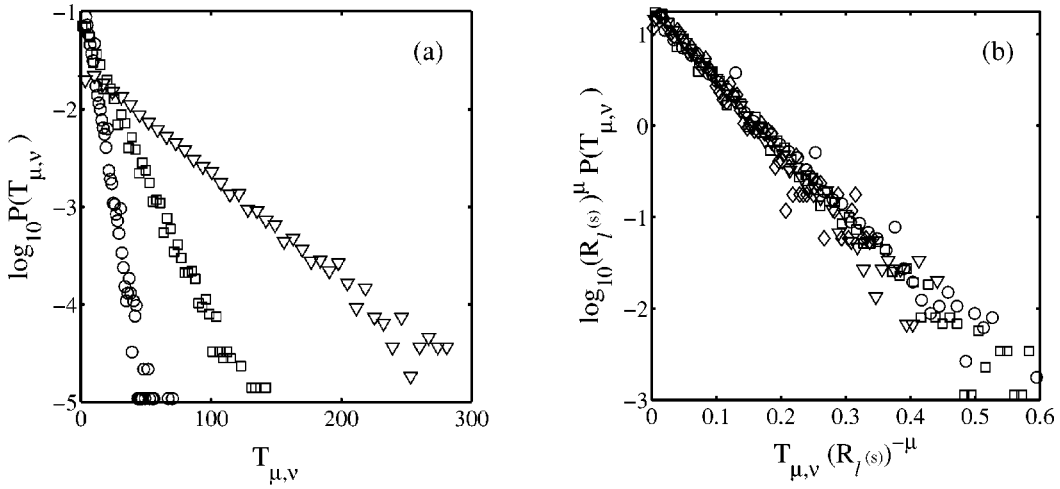

FIG. 2. Distributions for Tokunaga ratios for varying orders of absorbing stream and fixed side stream order of $\nu=2$ for the Scheidegger network. All quantities are dimensionless. In (a), we show examples of $T_{\mu,\nu}$ distributions for absorbing stream orders $\mu=4$ (circles), $\mu=5$ (squares), and $\mu=6$ (triangles). In (b), these distributions, as well as the $\mu=7$ case, are rescaled according to Eq. (10). The resulting ''data collapse'' gives a single distribution. For the Scheidegger model, $R_{l(s)}\simeq 3.00$.

the data is for the Mississippi. The rescaling is now by $R_{l(s)}$ rather than $R_{l(s)}^{-1}$, and Eq. (10) is improved to give

$$P(T_{\mu,\nu})=(R_{l(s)})^{\mu-\nu-1}P_T[T_{\mu,\nu}/(R_{l(s)})^{\mu-\nu-1}]. \quad (11)$$

The function P_T is a normalized exponential distribution independent of μ and ν,

$$P_T(z)=\frac{1}{\xi_t}e^{-z/\xi_t}, \quad (12)$$

where ξ_t is the characteristic number of side streams one order lower than the absorbing stream, i.e., $\xi_t=\langle T_1\rangle$. For the Mississippi, we observe $\xi_t\simeq 1.1$, whereas for the Scheidegger model we see $\xi_t\simeq 1.35$. As expected, the Tokunaga distribution is dependent only on $k=\mu-\nu$, so we can write

$$P(T_k)=(R_{l(s)})^{k-1}P_T[T_{\mu,\nu}/(R_{l(s)})^{k-1}], \quad (13)$$

with P_T as above.

V. CONNECTION TO STREAM SEGMENT LENGTHS AND RANDOMNESS

We have already examined the exponential distributions of stream segments lengths in Ref. [2], and here we develop its relationship with the Tokunaga distributions. Following Ref. [2], we write the distribution for stream segment lengths as

$$P(l_\mu^{(s)})=(R_{l(s)})^{-\mu+1}P_{l(s)}[l_\mu^{(s)}/(R_{l(s)})^{-\mu+1}], \quad (14)$$

where the function $P_{l(s)}$ is a normalized exponential distribution:

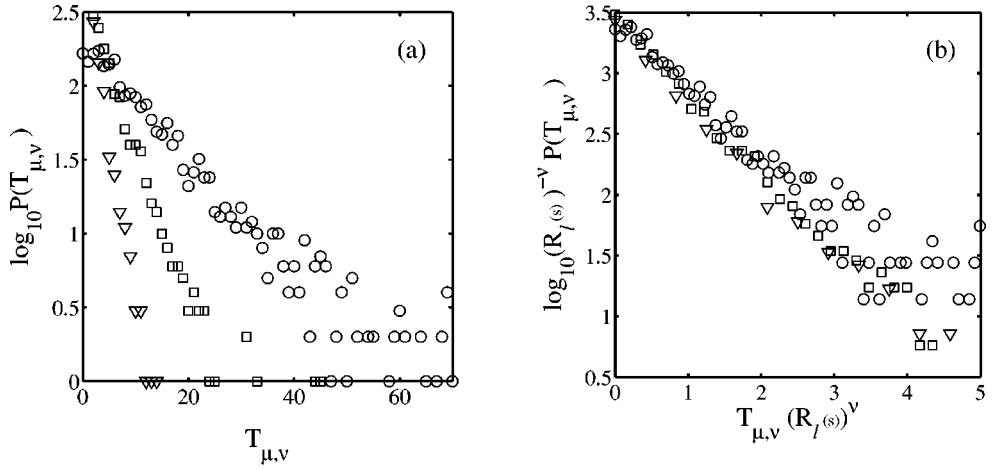

FIG. 3. Tokunaga distributions for varying side stream orders for the Mississippi river basin. All quantities are dimensionless. In both (a) and (b), the absorbing stream order is $\mu=5$, and the side stream orders are $\nu=2$ (circles), $\nu=3$ (squares), and $\nu=4$ (triangles). The raw distributions are shown in (a). In (b) the distributions are rescaled as per Eq. (11). For the Mississippi, the ratio is estimated to be $R_{l(s)}\simeq 2.40$ [2].

$$P_{l^{(s)}}(z)=\frac{1}{\xi_{l^{(s)}}}e^{-z/\xi_{l^{(s)}}}. \tag{15}$$

In a strictly self-similar network, $\xi_{l^{(s)}}$ is the characteristic length of first-order stream segments, i.e., $\xi_{l^{(s)}}=\langle l_1^{(s)}\rangle$. (Note that in Ref. [2] we use ξ for $\xi_{l^{(s)}}$ for ease of notation.) We qualify this by requiring the network to be exactly self-similar, because in real networks and most models this is certainly not the case. As should be expected, there are deviations from scaling for the largest and smallest orders. Therefore, $\xi_{l^{(s)}}$ is the characteristic size of a first-order stream as determined by scaling down the average lengths of those higher-order streams that are in the self-similar structure of the network. It is thus in general different from $\langle l_1^{(s)}\rangle$.

The connection between the characteristic number ξ_t and the length-scale $\xi_{l^{(s)}}$ follows from Eqs. (2), (4), and (9):

$$\xi_t=\rho_1 R_{l^{(s)}}\xi_{l^{(s)}}. \tag{16}$$

This presumes an exact scaling of drainage densities, and in the case where this is not so, ρ_1 would be chosen so that $(R_{l^{(s)}})^{\nu-1}\rho_1$ most closely approximates the higher order ρ_ν.

We now come to an interpretation of the exponential distribution as a composition of independent probabilities. Consider the example of stream segment lengths. We write $\tilde{p}_\mu$ as the probability that a stream segment of order μ meets with (and thereby terminates at) a stream of order at least μ. For simplicity, we assume that only one side stream, or none, may join a stream at any site. We also take the lattice spacing α to be unity, so that stream lengths are integers and therefore equate with the number of links between sites along a stream. For $\alpha\neq 1$, derivations similar to below will apply with $l_\mu^{(s)}$ replaced by $[l_\mu^{(s)}/\alpha]$, where [ ] denotes rounding to the nearest integer. Note that extra complications arise when the distances between neighboring sites are not uniform.

Consider a single instance of an order μ stream segment. The probability of this segment having a length $l_\mu^{(s)}$ is given by

$$P(l_\mu^{(s)})=\tilde{p}_\mu(1-\tilde{p}_\mu)^{l_\mu^{(s)}}, \tag{17}$$

where $\tilde{p}_\mu$ is the probability that an order μ stream segment terminates on meeting a stream of equal or higher order. We can re-express the above equation as

$$P(l_\mu^{(s)})\simeq\tilde{p}_\mu\exp\{-l_\mu^{(s)}\ln(1-\tilde{p}_\mu)^{-1}\}, \tag{18}$$

and, upon inspection of Eqs. (14) and (15), we make the identification

$$(R_{l^{(s)}})^{\mu-1}\xi_{l^{(s)}}=[-\ln(1-\tilde{p}_\mu)]^{-1}, \tag{19}$$

which has the inversion

$$\tilde{p}_\mu=1-e^{-1/(R_{l^{(s)}})^{\mu-1}\xi_{l^{(s)}}}. \tag{20}$$

For μ sufficiently large such that $\tilde{p}_\mu\ll 1$, we have the simplification

$$\tilde{p}_\mu\simeq 1/(R_{l^{(s)}})^{\mu-1}\xi_{l^{(s)}}. \tag{21}$$

We see that the probabilities satisfy the Horton-like scaling law

$$\tilde{p}_\mu/\tilde{p}_{\mu-1}=1/R_{l^{(s)}}. \tag{22}$$

Thus, we begin to see the element of randomness in our expanded description of network architecture. The termination of a stream segment by meeting a larger branch is effectively a spatially random process.

In addition, we observe that side streams are randomly placed along absorbing streams. Three new measures of stream length of use here are $l_{\mu,\nu}^{(s,b)}$, the distance from the beginning of an order μ absorbing stream to the first order ν side stream; $l_{\mu,\nu}^{(s,i)}$, the distance between any two adjacent internal order ν side streams along an order μ absorbing stream; and $l_{\mu,\nu}^{(s,e)}$, the distance from the last order ν side stream to the end of an order μ absorbing stream. We observe in both the Scheidegger model and real data, the distributions of $l_{\mu,\nu}^{(s,b)}$, $l_{\mu,\nu}^{(s,i)}$, and $l_{\mu,\nu}^{(s,e)}$ to be well approximated by exponential distributions and, moreover, to be indistinguishable [17]. This indicates that drainage density is independent of relative position of tributaries along an absorbing stream.

VI. JOINT VARIATION OF TOKUNAGA RATIOS AND STREAM SEGMENT LENGTH

We have so far observed that the individual distributions of $l_\mu^{(s)}$ and $T_{\mu,\nu}$ are exponential, and that they are related via the side-stream density ρ_ν. However, this is not an exact relationship. For example, given a collection of stream segments with a fixed length $l_\mu^{(s)}$ we expect to find fluctuations in the corresponding Tokunaga ratios $T_{\mu,\nu}$.

To investigate this further we now consider the joint variation of $T_{\mu,\nu}$ with $l_\mu^{(s)}$ from a number of perspectives. After discussing the full joint probability distribution $P(T_{\mu,\nu},l_\mu^{(s)})$, we then focus on the quotient $v=T_{\mu,\nu}/l_\mu^{(s)}$ and its reciprocal $w=l_\mu^{(s)}/T_{\mu,\nu}$. The latter two quantities are measures of drainage density and intertributary length for an individual absorbing stream.

A. Joint probability distribution

We build the joint distribution of $P(T_{\mu,\nu},l_\mu^{(s)})$ from our conception that stream segments are randomly distributed throughout a basin. In Eq. (17), we have the probability of a stream segment terminating after $l_\mu^{(s)}$ steps. We need to incorporate into this form the probability that the stream segment also has $T_{\mu,\nu}$ order ν side streams. Since we assume placement of these side streams to be random, we modify Eq. (17) to find

$$P(l_\mu^{(s)},T_{\mu,\nu})=\tilde{p}_\mu\binom{l_\mu^{(s)}-1}{T_{\mu,\nu}}p_\nu^{T_{\mu,\nu}}(1-p_\nu-\tilde{p}_\mu)^{l_\mu^{(s)}-T_{\mu,\nu}-1}, \tag{23}$$

where $\binom{n}{k}=n!/k!(n-k)!$ is the binomial coefficient, and p_ν is the probability of absorbing an order ν side stream. The extra p_ν appears in the last factor $(1-p_\nu-\tilde{p}_\mu)$ because this

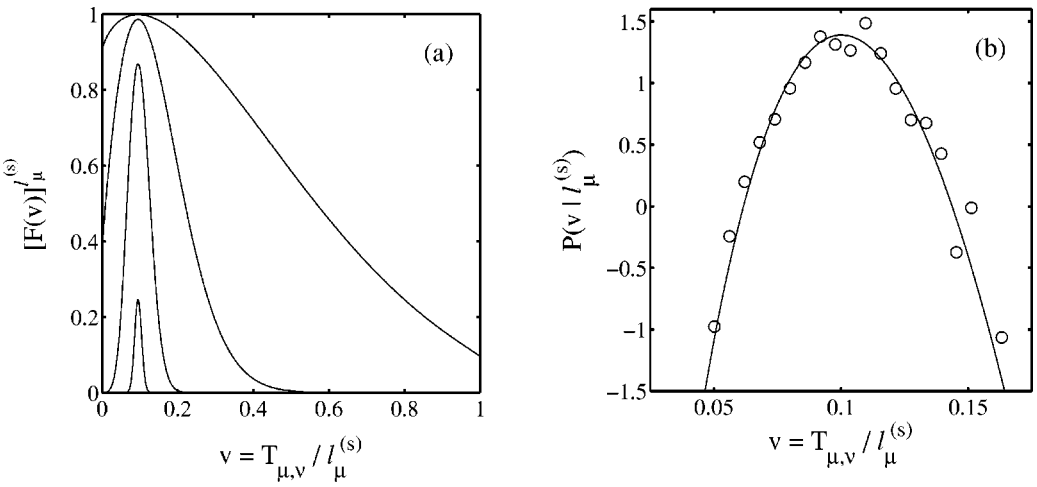

FIG. 4. Form of the joint distribution of Tokunaga ratios and stream segment lengths. The distribution is given in Eq. (25), and is built around the function $F(v=T_{\mu,\nu}/l_\mu^{(s)})$ given in Eq. (26). Lengths are in terms of arbitrary lattice units, and all other quantities are dimensionless. Shown in (a) is $[F(v)]^{l_\mu^{(s)}}$ for $l_\mu^{(s)}=1$, 10, 100, and 1000. Increasing $l_\mu^{(s)}$ corresponds to the focusing of the shape. In (b), the distribution $P(T_{\mu,\nu}|l_\mu^{(s)}\simeq 340)$ is compared between theory (smooth curve) and data from the Scheidegger model (circles). The Scheidegger model data is compiled for a range of values of $l_\mu^{(s)}$ rescaled as per Eq. (27).

term is the probability that at a particular site the stream segment neither terminates nor absorbs an order ν side stream. Also, it is simple to verify that the sum over $l_\mu^{(s)}$ and $T_{\mu,\nu}$ of the probability in Eq. (18) returns unity.

While Eq. (18) does precisely describe the joint distribution $P(l_\mu^{(s)},T_{\mu,\nu})$, it is somewhat cumbersome to work with. We therefore find an analogous form defined for continuous rather than discrete variables. We simplify our notation by writing $p=p_\nu$, $q=(1-p_\nu-\tilde{p}_\mu)$ and $\tilde{p}=\tilde{p}_\mu$. We also replace $(l_\mu^{(s)},T_{\mu,\nu})$ by (x, y) where now $x,y\in[\mathbb{R}]$. Note that $0\leqslant y\leqslant x-1$, since the number of side streams cannot be greater than the number of sites within a stream segment.

Equation (18) becomes

$$P(x,y)=N\tilde{p}\frac{\Gamma(x)}{\Gamma(y+1)\Gamma(x-y)}(p)^y(q)^{x-y-1}, \qquad (24)$$

where we have used $\Gamma(z+1)=z!$ to generalize the binomial coefficient. We have included the normalization N to account for the fact that we have moved to continuous variables, and the resulting probability may not be cleanly normalized. Also we must allow that $N=N(p,\tilde{p})$ and we will be able to identify this form more fully later on. Using Stirling's approximation [18], that $\Gamma(z+1)\sim\sqrt{2\pi}z^{z+1/2}e^{-z}$, we then have

$$\begin{aligned}P(x,y)&=N\tilde{p}p^yq^{x-y-1}\frac{1}{\sqrt{2\pi}}\frac{(x-1)^{x-3/2}}{y^{y+1/2}(x-y-1)^{x-y-1/2}}\\&=N\frac{\tilde{p}}{\sqrt{2\pi q}}p^yq^{x-y}(x-1)^{-1/2}\left(\frac{y}{x-1}\right)^{-y-1/2}\\&\quad\times\left(1-\frac{y}{x-1}\right)^{-x+y+1/2}\\&\simeq N'x^{-1/2}[F(y/x)]^x, \qquad (25)\end{aligned}$$

where we have absorbed N and all terms involving only p and $\tilde{p}$ into the prefactor $N'=N'(p,\tilde{p})=N\tilde{p}/(\sqrt{2\pi q})$. We have also assumed x is large such that $x-1\simeq x$ and $1\gg 1/x\simeq 0$.

The function $F(v=y/x)=F(v;p,q)$ identified above has the form

$$F(v)=\left(\frac{1-v}{q}\right)^{-(1-v)}\left(\frac{v}{p}\right)^{-v}, \qquad (26)$$

where $0<v<1$. Note that for fixed x, the conditional probability $P(y|x)$ is proportional to $[F(y/x)]^x$. Figure 4(a) shows $[F(v)]^x$ for a range of powers x. The basic function has a single peak situated near $v=p$. For increasing x which corresponds to increasing $l_\mu^{(s)}$, the peak becomes sharper approaching (when normalized) a delta function, i.e., $\lim_{x\to\infty}[F(v)]^x=\delta(v-p)$.

Figure 4(b) provides a comparison between data for the Scheidegger model and the analytic form of $P(l_\mu^{(s)},T_{\mu,\nu})$. For this example, $\mu=6$ and $\nu=2$ which corresponds to $p\simeq 0.10$, $q\simeq 0.90$, and $\tilde{p}\simeq 0.001$ (using the results of Sec. V). The smooth curve shown is the conditional probability $P(y|X)$ for the example value of $X=l_\mu^{(s)}\simeq 340$ following from Eq. (25). From simulations, we obtain a discretized approximation to $P(l_\mu^{(s)},T_{\mu,\nu})$. For each fixed $x=l^{(s)}$ in the range $165\lesssim l_\mu^{(s)}\lesssim 345$, we rescale the data using the following, derived from Eq. (25):

$$P(X,y)=N'X^{-1/2}[N'^{-1}x^{1/2}P(x,y)]^{X/x}. \qquad (27)$$

The rescaled data are then combined, binned, and plotted as circles in Fig. 4(b), showing excellent agreement with the theoretical curve.

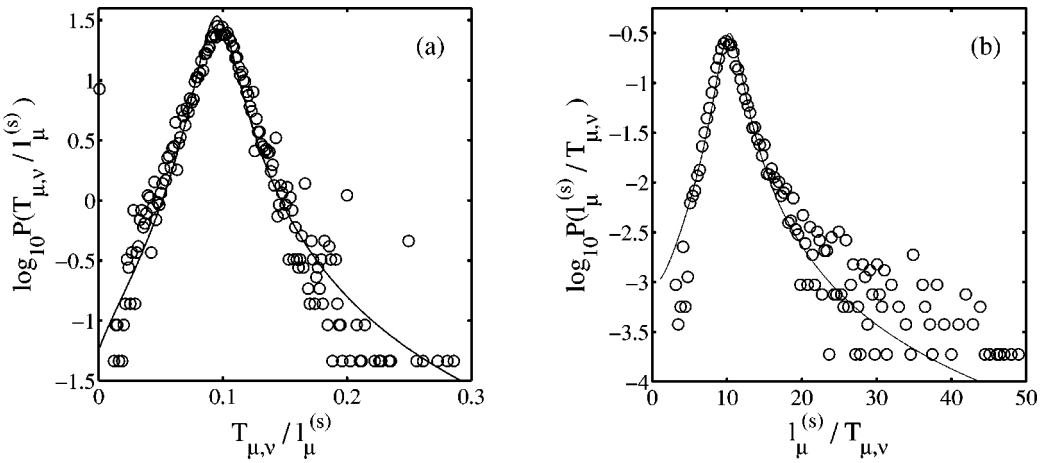

FIG. 5. Comparison of theory with measurements of average intertributary distances for the Scheidegger model. Dimensions are as per Fig. 4. The data in both (a) and (b) are for the case of order $\nu=2$ side streams and order $\mu=6$ absorbing streams. In (a), the distribution of $v=T_{\mu,\nu}/l_\mu^{(s)}$ obtained from the Scheidegger model (circles) is compared with the smooth curved predicted in Eq. (32). The same comparison is made for the reciprocal variable $w=l_\mu^{(s)}/T_{\mu,\nu}$, the predicted curve being given in Eq. (33).

B. Distributions of side branches per unit stream length

Having obtained the general form of $P(l_\mu^{(s)},T_{\mu,\nu})$, we now delve further into its properties by investigating the distributions of the ratio $v=T_{\mu,\nu}/l_\mu^{(s)}$ and its reciprocal w. The quantity $T_{\mu,\nu}/l_\mu^{(s)}$ is the number of side streams per length of a given absorbing stream, and when averaged over an ensemble of absorbing streams gives

$$\langle T_{\mu,\nu}/l_\mu^{(s)}\rangle=\rho_\nu. \tag{28}$$

Accordingly, the reciprocal $l_\mu^{(s)}/T_{\mu,\nu}$ is the average separation of side streams of order ν.

First, we derive $P(T_{\mu,\nu}/l^{(s)})$ from $P(l_\mu^{(s)},T_{\mu,\nu})$. We then consider some intuitive rescalings which will allow us to deduce the form of the normalization $N(p,q)$.

We rewrite Eq. (25) as

$$P(x,y)=N'x^{-1/2}\exp\{-x\ln[-F(y/x)]\}. \tag{29}$$

We transform (x,y) to the modified polar coordinate system described by (u,v) with the relations

$$u^2=x^2+y^2 \quad \text{and} \quad v=y/x. \tag{30}$$

The inverse relations are $x=u/(1+v^2)$ and $y=uv/(1+v^2)$ and we also have $dx\,dy=x\,du\,dv$. Equation (31) leads to

$$P(u,v)=N'\left(\frac{u}{1+v^2}\right)^{1/2}\exp\left\{-\frac{u}{1+v^2}\ln[-F(v)]\right\}. \tag{31}$$

To find $P(v)$ we integrate out over the radial dimension u:

$$\begin{aligned}P(v)&=\int_{u=0}^{\infty}du\,P(u,v)\\&=N'\int_{u=0}^{\infty}du\left(\frac{u}{1+v^2}\right)^{1/2}\exp\left\{-\frac{u}{1+v^2}\ln[-F(v)]\right\}\\&=N'(1+v^2)\{\ln[-F(v)]\}^{-3/2}\int_{z=0}^{\infty}dz\,z^{1/2}e^{-z}\\&=N''\frac{1+v^2}{\{\ln[-F(v)]\}^{3/2}}.\end{aligned} \tag{32}$$

Here, $N''=N'\Gamma(3/2)=N'\sqrt{\pi}/2$, and we have used the substitution $z=u/(1+v^2)\ln[-F(v)]$.

The distribution for $w=l_\mu^{(s)}/T_{\mu,\nu}=1/v$ follows simply from Eq. (32), and we find

$$P(w)=N''\frac{1+w^2}{w^4\{\ln[-F(1/w)]\}^{3/2}}. \tag{33}$$

Figures 5(a) and 5(b) compare the predicted forms of $P(v)$ and $P(w)$ with data from the Scheidegger model. In both cases, the data are for order $\nu=2$ side streams being absorbed by streams of order $\mu=6$. Note that both distributions show an initially exponential-like decay away from a central peak.

Finally, we quantify how changes in the orders μ and ν affect the width of the distributions by considering some natural rescalings. Because the average length of $l_\mu^{(s)}$ increases by a factor $R_{l(s)}$ with μ, the typical number of side streams increases by the same factor. Since we can decompose $l_\mu^{(s)}$ as

$$l_\mu^{(s)}=l_{\mu,\nu}^{(s,b)}+l_{\mu,\nu}^{(s,i)}+\cdots+l_{\mu,\nu}^{(s,i)}+l_{\mu,\nu}^{(s,e)}, \tag{34}$$

where there are $T_{\mu,\nu}-1$ instances of $l_{\mu,\nu}^{(s,i)}$, $l_\mu^{(s)}$ becomes better and better approximated by $(T_{\mu,\nu}+1)\langle l_{\mu,\nu}^{(s,i)}\rangle$.

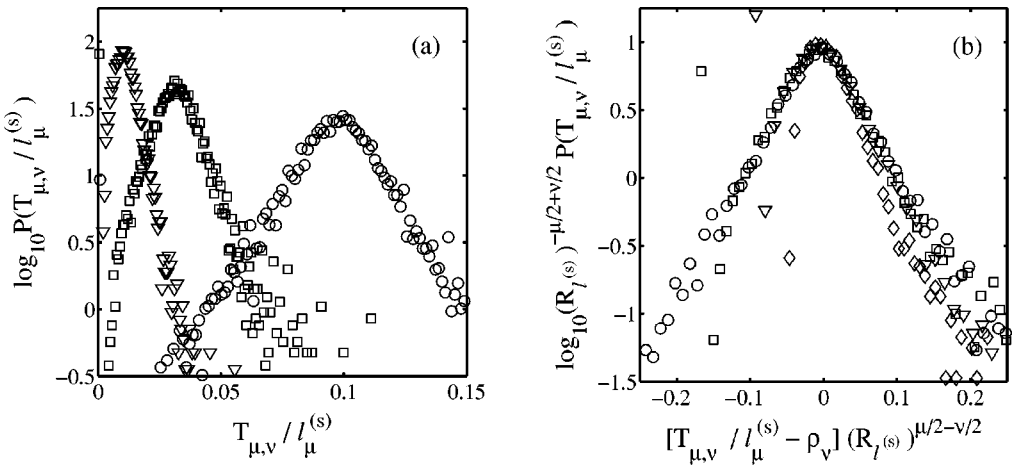

FIG. 6. Distributions of the number of side streams per unit length for the Scheidegger model with ν, the order of side streams, varying. Dimensions are as per Fig. 4, with the addition that the drainage density ρ_ν is in inverse lattice units. For both (a) and (b), the absorbing stream order is $\mu=6$. Shown in (a) are the unrescaled distributions for $\nu=2$ (circles), $\nu=3$ (squares), and $\nu=4$ (triangles). Note that as ν increases, the mean number of side streams decreases as do the fluctuations. The distributions in (a), together with the distribution for $\nu=5$ (diamonds), are shown rescaled in (b) as per Eq. (37).

Hence the distribution of $T_{\mu,\nu}/l_\mu^{(s)}$ peaks up around ρ_ν as μ increases, the typical width reducing by a factor of $1/\sqrt{R_{l(s)}}$ for every step in μ. We therefore have

$$P(T_{\mu,\nu}/l_\nu^{(s)}) = (R_{l(s)})^{\mu/2} G_1\{[T_{\mu,\nu}/l_\nu^{(s)} - \rho_\nu](R_{l(s)})^{\mu/2}\}, \tag{35}$$

where the function is similar to the form of $P(v)$ given in Eq. (32). The mean drainage density of ρ_ν has been subtracted to center the distribution.

We are able to generalize this scaling form of the distribution further by taking into account side stream order. Figures 6(a) and 6(b), respectively, show the unrescaled and rescaled distributions of $T_{\mu,\nu}/l_\mu^{(s)}$ with ν allowed to vary. This particular example taken from the Scheidegger model is for $\mu=6$, and the range $\nu=1-5$. Since ν is now changing, the centers are situated at the separate values of the ρ_ν. Also, the typical number of side streams changes with order ν so the widths of the distributions dilate as for the varying μ case by a factor $\sqrt{R_{l(s)}}$. Note that the rescaling works well for $\nu=2,\ldots,5$ but not $\nu=1$. As we have noted, deviations from scaling from small orders are to be expected. We now write

$$P(T_{\mu,\nu}/l_\nu^{(s)})(R_{l(s)})^{-\nu/2} G_2\{[T_{\mu,\nu}/l_\nu^{(s)} - \rho_\nu](R_{l(s)})^{-\nu/2}\}, \tag{36}$$

where, again, $G_2(z)$ is similar in form to $P(v)$.

We find the same rescalings apply for the Mississippi data. For example, Fig. 7(a) shows unrescaled distributions of $T_{\mu,\nu}/l_\nu^{(s)}$ for varying ν. Figure 7(b) then shows reasonable agreement with the form of Eq. (36). In this case, the Scheidegger model clearly affords valuable guidance in our in-

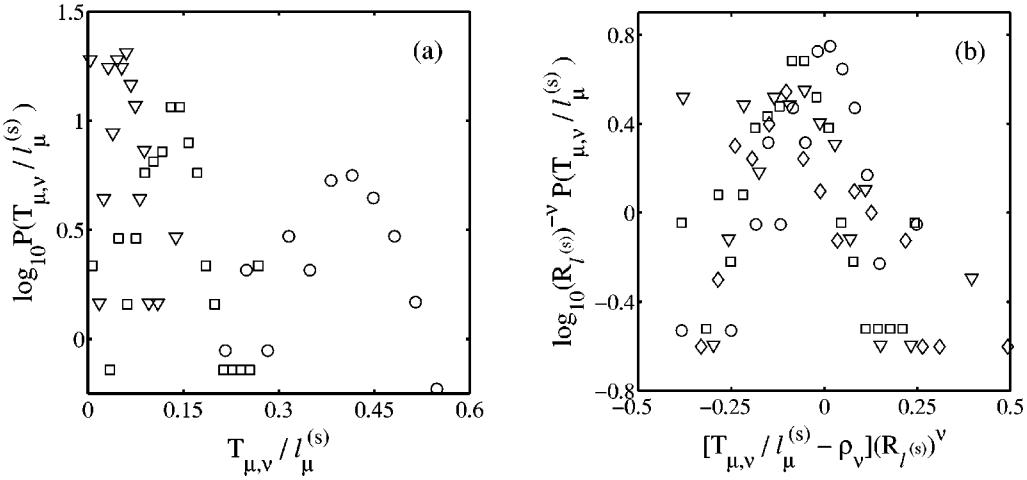

FIG. 7. Tokunaga statistics for the Mississippi river basin. The distributions are as per Fig. 6(a), distributions of number of side streams per unit length, with ν, the order of side streams, varying. The dimensions of length and reciprocal density $1/\rho_\nu$ are now given in meters, and all other quantities are dimensionless. The absorbing stream order is $\mu=7$, and the individual distributions correspond to $\nu=2$ (circles), $\nu=3$ (squares), and $\nu=4$ (triangles). Rescalings of the distributions shown in (a), along with that for $\nu=5$ (diamonds), are found in (b). Reasonable agreement with Eq. (37) is observed.

vestigations of real river networks. The ratio $R_{l^{(s)}}=2.40$ was calculated from an analysis of $l_\omega^{(s)}$ and l_ω. The density $\rho_2 \simeq 0.0004$ was estimated directly from the distributions of $T_{\mu,\nu}/l_\nu^{(s)}$, and means that approximately four second-order streams appear every ten kilometers.

Combining Eqs. (35) and (36), we obtain the complete scaling form

$$P(T_{\mu,\nu}/l_\nu^{(s)}) = (R_{l^{(s)}})^{(\mu-\nu-1)/2} G\{[T_{\mu,\nu}/l_\nu^{(s)} - \rho_\nu] \times (R_{l^{(s)}})^{(\mu-\nu-1)/2}\}. \quad (37)$$

As per G_1 and G_2, the function G is similar in form to $P(v)$.

The above scaling form makes intuitive sense but is not obviously obtained from an inspection of Eq. (32). We therefore examine $P(v)$ by determining the position and magnitude of its maximum. Rather than solve $P'(v)=0$ directly, we find an approximate solution by considering the argument of the denominator, $-\ln F(v)$, with $F(v)$ given in Eq. (26). Since the numerator of $P(v)$ is $1+v^2$, and the maximum occurs for small v this is a justifiable step. Setting $dF/dv = 0$, we thus have

$$-\ln\frac{1-v}{q} + \ln vp = 0, \quad (38)$$

which gives $v_m = p/(q+p) = p/(1-\tilde{p})$. Note that for $\tilde{p} \ll 1$, we have $v_m \simeq p$.

Substituting $v = v_m = p/(1-\tilde{p})$ into Eq. (32), we find

$$P(v_m) \simeq N'' \tilde{p}^{-3/2} = N \tilde{p}^{-1/2} 2^{-3/2}, \quad (39)$$

presuming $p^2 \ll 1$ and $q \simeq 1$. Returning to the scaling form of Eq. (37), we see that the $\tilde{p}^{-1/2}$ factor in Eq. (39) accounts for the factors of $(R_{l^{(s)}})^{\mu/2}$ since $\tilde{p} = \tilde{p}_\mu$ scales from level to level by the ratio $R_{l^{(s)}}$. We therefore find the other factor $(R_{l^{(s)}})^{\nu/2}$ of Eq. (37) gives $N = cp^{1/2}$, where c is a constant. Since $p = p_\nu$, it is the only factor that can provide this variation. We thus have found the variation with stream order of the normalization N, and have fully characterized $P(x,y)$, the continuum approximation of $P(l_\mu^{(s)}, T_{\mu,\nu})$.

VII. CONCLUDING REMARKS

This paper provides an investigation of detailed river network architecture as viewed in planform. We identify the self-similarity of a form of drainage density as the essence of the average connectivity and structure of networks. From previous work in Ref. [5], we understand this to be a base from which all river network scaling laws may obtained.

We extend the description of tributary structure provided by Tokunaga's law to find that side stream numbers are distributed exponentially. This in turn is seen to follow from the fact that the length of stream segments are themselves exponentially distributed. We interpret this to be consequence of randomness in the spatial distribution of stream segments. Furthermore, the presence of exponential distributions indicates that fluctuations in variables are significant being on the order of mean values. For the example of stream segment lengths, we thus identify $\xi_{l^{(s)}}$, a single parameter needed to describe all moments. This is simply related to ξ_t, which describes the distributions of Tokunaga ratios. The exponential distribution becomes the null hypothesis for the distributions of these variables to be used in the examination of real river networks.

We are able to discern the finer details of the connection between stream segment length and tributary numbers. Analysis of the placement of side streams along a stream segment again reveals exponential distributions. We are then able to postulate a joint probability distribution for stream segment lengths and the Tokunaga ratios. The functional form obtained agrees well with both model and real network data. By further considering distributions of the number of side streams per unit length of individual stream segments, we are able to capture how variations in the separation of side streams are averaged out along higher-order absorbing streams.

We end with a brief comment on the work of Cui, Williams, and Kuczera [13], who recently also proposed a stochastic generalization of Tokunaga's law. They postulate that the underlying distribution for the $T_{\mu,\nu}$ is a negative binomial distribution. One parameter additional to T_1 and R_T, α, was introduced to reflect ''regional variability,'' i.e., statistical fluctuations in network structure. This is in the same spirit as our identification of a single parameter ξ_t. However, our work disagrees on the nature of the underlying distribution of $T_{\mu,\nu}$. We have consistently observed exponential distributions for $T_{\mu,\nu}$ in both model and real networks.

In closing, by finding randomness in the spatial distribution of stream segments, we have arrived at the most basic description of river network architecture. Understanding the origin of the exact values of quantities such as drainage density remains an open problem.

ACKNOWLEDGMENTS

The authors would like to thank J. S. Weitz for useful discussions. This work was supported in part by NSF Grant No. EAR-9706220 and Department of Energy Grant No. DE FG02-99ER 15004.

[1] P. S. Dodds and D. H. Rothman, first paper, Phys. Rev. E **63**, 016115 (2000).

[2] P. S. Dodds and D. H. Rothman, preceding paper, Phys. Rev. E **63**, 016116 (2000).

[3] A. Maritan, A. Rinaldo, R. Rigon, A. Giacometti, and I. Rodríguez-Iturbe, Phys. Rev. E **53**, 1510 (1996).

[4] I. Rodríguez-Iturbe and A. Rinaldo, *Fractal River Basins: Chance and Self-Organization* (Cambridge University Press, Cambridge, 1997).

[5] P. S. Dodds and D. H. Rothman, Phys. Rev. E **59**, 4865

(1999).
[6] P. S. Dodds and D. H. Rothman, Annu. Rev. Earth Planet Sci. **28**, 571 (2000).
[7] E. Tokunaga, Geophys. Bull. Hokkaido Univ. **15**, 1 (1966).
[8] E. Tokunaga, Geogr. Rep., Tokyo Metrop. Univ. **13**, 1 (1978).
[9] E. Tokunaga, Trans. Jpn. Geomorphol. Union, **5**, 71 (1984).
[10] A. E. Scheidegger, Bull. Int. Assoc. Sci. Hydrol. **12**, 15 (1967).
[11] R. E. Horton, Bull. Geol. Soc. Am. **56**, 275 (1945).
[12] A. N. Strahler, EOS Trans. AGU **38**, 913 (1957).
[13] G. Cui, B. Williams, and G. Kuczera, Water Resour. Res. **35**, 3139 (1999).
[14] D. L. Turcotte, J. D. Pelletier, and W. I. Newman, J. Theor. Biol. **193**, 577 (1998).
[15] S. D. Peckham, Water Resour. Res. **31**, 1023 (1995).
[16] The network for the Mississippi was extracted from a topographic dataset constructed from 3-arcsec USGS Digital Elevation Maps, decimated by averaging to approximately 1000-m horizontal resolution (www.usgs.gov). At this grid scale, the Mississippi was found to be an order $\Omega = 11$ basin.
[17] P. S. Dodds, Ph.D. thesis, Massachusetts Institute of Technology, 2000.
[18] C. M. Bender and S. A. Orszag, *Advanced Mathematical Methods for Scientists and Engineers*, International Series in Pure and Applied Mathematics (McGraw-Hill, New York, 1978).